THE JOURNAL OF PHYSICAL CHEMISTRY B

Article

pubs.acs.org/JPCB

Molecular Dynamics Simulations of Membrane–Sugar Interactions

Jon Kapla,[†] Jakob Wohlert,[‡] Baltzar Stevensson,[†] Olof Engström,[§] Göran Widmalm,[§] and Arnold Maliniak*[,†]

[†]Department of Materials and Environmental Chemistry, Arrhenius Laboratory, Stockholm University, SE-106 91 Stockholm, Sweden

[‡]Wallenberg Wood Science Center, Royal Institute of Technology, SE-100 44 Stockholm, Sweden

[§]Department of Organic Chemistry, Arrhenius Laboratory, Stockholm University, SE-106 91 Stockholm, Sweden

Supporting Information

ABSTRACT: It is well documented that disaccharides in general and trehalose (TRH) in particular strongly affect physical properties and functionality of lipid bilayers. We investigate interactions between lipid membranes formed by 1,2-dimyristoyl-*sn*-glycero-3-phosphocholine (DMPC) and TRH by means of molecular dynamics (MD) computer simulations. Ten different TRH concentrations were studied in the range w_{TRH} = 0–0.20 (w/w). The potential of mean force (PMF) for DMPC bilayer–TRH interactions was determined using two different force fields, and was subsequently used in a simple analytical model for description of sugar binding at the membrane interface. The MD results were in good agreement with the predictions of the model. The net affinities of TRH for the DMPC bilayer derived from the model and MD simulations were compared with experimental results. The area per lipid increases and the membrane becomes thinner with increased TRH concentration, which is interpreted as an intercalation effect of the TRH molecules into the polar part of the lipids, resulting in conformational changes in the chains. These results are consistent with recent experimental observations. The compressibility modulus related to the fluctuations of the membrane increases dramatically with increased TRH concentration, which indicates higher order and rigidity of the bilayer. This is also reflected in a decrease (by a factor of 15) of the lateral diffusion of the lipids. We interpret these observations as a formation of a glassy state at the interface of the membrane, which has been suggested in the literature as a hypothesis for the membrane–sugar interactions.

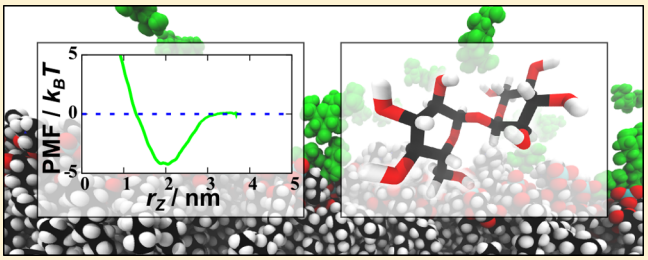

INTRODUCTION

Understanding biological membrane–sugar interactions has attracted considerable attention in the scientific literature. It is because disaccharides in general,[1−4] and trehalose (TRH) in particular, have stabilizing effects on biological membranes under extreme thermal and mechanical conditions.[5] These effects are particularly important during the process of dehydration.[6] The effect of sugars preserving the cell structure and biological function is well-known; the detailed molecular mechanisms for these effects are, however, not clear.

Two general models for description of membrane–sugar interactions have been proposed: (i) a preferential exclusion model, where sugars are excluded from the vicinity of the lipid membrane, thus preserving the natural hydration shell of the bilayer;[4] and (ii) a preferential interaction model. In the latter model, in turn, three main hypotheses have been suggested: (a) water replacement,[7] where sugars substitute water molecules around polar parts of the lipid membrane; (b) the water-entrapment hypothesis,[8−10] resting on the assumption that the sugars interact strongly with both lipids and water, which increases favorable hydration near the membrane interface; and finally (c) the vitrification hypothesis,[11−13] where the sugars act as vitrifying agents by, in analogy with "caramelization" of food, forming a glassy structure that protects the membrane from mechanical stress. There are, however, clear indications that the different hypotheses are not mutually exclusive.[11,14−16]

In the present investigation, we use molecular dynamics (MD) computer simulations for analysis of interactions between a 1,2-dimyristoyl-*sn*-glycero-3-phosphocholine (DMPC) bilayer and trehalose. Computer simulation is a powerful tool for investigations of the detailed picture of complex biological systems and several studies of lipid bilayer–trehalose interactions have been reported previously.[3,5,17−21] The study is carried out for a lipid bilayer consisting of 128 DMPC and ten different trehalose concentrations: 0, 20, 30, 40, 80, 140, 170, 200, 230, and 260 TRH molecules (labeled as TRH*N*, where *N* is the total number of TRH molecules), corresponding to a maximum trehalose content of w_{TRH} = 0.20 (w/w). A representative snapshot, created using the VMD software,[22] of the DMPC bilayer with trehalose is displayed in Figure 1. We focus on the details of membrane–sugar interactions and physical properties of the bilayer, which in turn have strong implications on functionality of the membrane. In a recent experimental study,[4] the net affinity of

Received: March 8, 2013
Revised: May 7, 2013
Published: May 10, 2013

   dx.doi.org/10.1021/jp402385d | *J. Phys. Chem. B* 2013, 117, 6667–6673

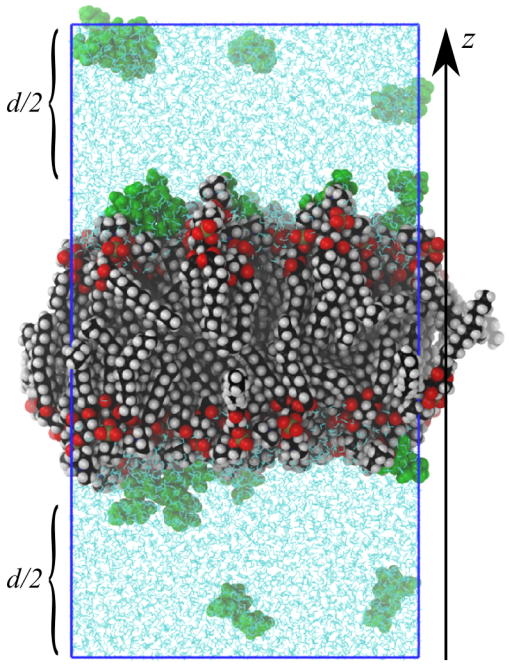

Figure 1. Snapshot of an equilibrated DMPC bilayer with trehalose molecules (green) after 100 ns of MD simulation. Oxygen atoms in DMPC are colored red and the height of the water phase is labeled *d*.

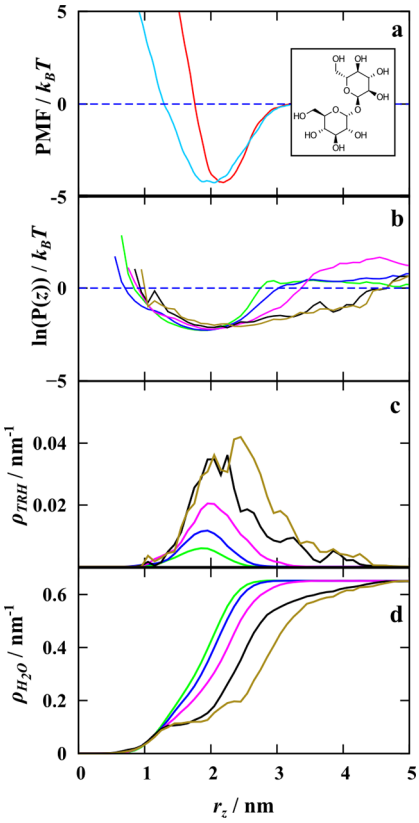

Figure 2. Schematic structure of the trehalose (TRH) molecule and the distance from the bilayer center dependence of several properties: (a) the potential of mean force (PMF) for interactions between TRH and DMPC bilayer, calculated by dragging two TRH molecules (one on each side of the membrane) through the bilayer using GROMOS (red) and AMBER (cyan) force fields; (b) the PMF calculated by inverting selected probability distribution functions: TRH20 (green), TRH40 (blue) TRH80 (magenta), TRH170 (black), and TRH230 (yellow); (c) probability distribution functions for TRH for selected concentrations, coloring as in (b); and (d) probability distribution functions for water for selected concentrations, coloring as in (b). Note that the distributions in (c) and (d) are normalized to the number of molecules. Panels (b–d) correspond to the molecular dynamics simulations carried out using the AMBER force field.

TRH for a fully hydrated lipid bilayer was investigated, and the results were interpreted invoking attraction and repulsion of sugar. These phenomena were observed at low and high sugar contents, respectively, and interpreted as reconciliation of conflicting views on membrane–sugar interactions. Here we use a simple quantitative two-state model for analysis of the interactions in the fully hydrated system,[4] and apply the same model to a substantially more dehydrated system (our MD simulations). In addition, in the dehydrated system a drastic change of mechanical properties, such as area compressibility modulus, of the lipid bilayer is observed upon increased TRH concentration.

MODELS

Membrane–Sugar Interaction Model. In order to quantitatively describe the membrane–TRH interactions, we use a simple two-state model with binding probabilities for bound (P_B) and free (P_F) solutes: $P_B/P_F = z_B/z_F$, with $z_F = d/2$, where d is the thickness of the solvent layer (see Figure 1), and

$$z_B = \int_0^{z_C} e^{-W(z)/k_BT}\, dz \tag{1}$$

where $W(z)$ is the work function or the potential of mean force (PMF). The parameters z_B and z_F are proportional to the integrated particle densities and correspond to the number of particles in the two regions. Using the PMF (AMBER) function displayed in Figure 2a and the limit for the bound region, z_C = 3 nm, the parameter z_B = 43 nm is obtained from eq 1.

The differential equation for the binding probability becomes

$$\frac{dN_B}{dN} = P_B = \frac{V_B}{V_F + V_B} = \frac{A - BN_B}{[C - D(N - N_B)] + [A - BN_B]} \tag{2}$$

where N_B is the number of bound molecules out of total N TRH molecules, with V_B and V_F being the volumes of the bound and free phases, respectively. The parameters are defined as $A = z_B N_L A_L$, the total amount of bound volume available; $B = z_B a_0$ is the excluded volume per TRH molecule in the bound state; $C = z_F N_L A_L$ is the total available free (solvent) volume; and $D = v_0$ is the excluded volume per TRH in the free phase (0.84 nm^3, derived from the solubility of TRH[23]). The solution of eq 2 is given by

$$N = -\frac{C}{D}\left(1 - \frac{B}{A}N_B\right)^{-D/B} - N_B + \frac{C}{D} \tag{3}$$

The solution depends on C/D, which reflects the total number of free sites, A/B, which is the total number of binding sites, and D/B, which is the ratio between the excluded volumes of the bound and free phases, respectively. Furthermore, the parameters N_L, A_L, a_0, and v_0 are the number of lipids, area per lipid, area per TRH molecule in the bound phase, and volume of a TRH molecule in the free phase, respectively. With some rearrangements, eq 3 becomes

dx.doi.org/10.1021/jp402385d | J. Phys. Chem. B 2013, 117, 6667–6673

$$N = n_F\left[1 - \frac{N_B}{n_F} - \left(1 - \frac{N_B}{n_B}\right)^{-v_B/v_F}\right] \quad (4)$$

where n_F is the (total) number of free sites, n_B is the (total) number of binding sites, and v_B and v_F are the free volumes of the bound and free TRH states, respectively. The model depends implicitly (through both n_B and v_B) on a_0, which is the free area of a bound TRH molecule.

RESULTS AND DISCUSSION

In Figure 2a, the potentials of mean force calculated using two different force fields are displayed: in addition to the AMBER based force field used in all the other simulations in the present study, a preliminary test was performed employing the GROMOS-derived interaction models.[24,25] The PMFs were calculated by dragging two TRH molecules (one on each side of the bilayer) through the membrane using a penalty potential in one dimension.

The TRH molecules retain their complete motional freedom except for the translational motion in the direction parallel to the normal of the bilayer that is constrained, using an umbrella-type potential, acting on the center of mass of the solute. The two PMFs in Figure 2a show very similar locations and depths of the potential energy minima. The minima are located at 2 nm which, on average, corresponds to the positions of the carbonyl oxygens in DMPC. The PMFs can also be derived from the probability distribution function for finding a TRH molecule at a given distance from the bilayer center. The PMFs are displayed in Figure 2b, whereas the corresponding distributions for TRH20, TRH40, TRH80, TRH170 and TRH230 are shown in Figure 2c. The distributions are normalized so that the integral corresponds to the number of TRH molecules in the sample. Clearly, the PMFs calculated from the distribution functions exhibit significantly shallower minima compared to the single particle PMFs displayed in Figure 2a. The location of the minima is, however, very similar to that in Figure 2a, whereas the accessible region for TRH molecules in the membrane is significantly increased. This is consistent with one of the hypotheses suggested for the membrane–sugar interactions where water is replaced by TRH molecules.

To quantitatively describe membrane–TRH interactions, we use the simple two-state model (see the Models section) in which TRH molecules are either free or bound. The solute molecules are noninteracting, but excluded volume effects in both states are accounted for. This leads to the relation between the total number of TRH (N) and the number of bound TRH (N_B) according to eq 4.

In Figure 3, the number of bound TRH molecules as a function of total number of molecules is displayed for two values of the parameter a_0, 0.50 and 0.65 nm^2, and the area per lipid (A_L) is approximated to 0.64 nm^2. Both values of a_0 are reasonably consistent with the hydrodynamic volume of the TRH molecule as recently determined from deuterium NMR relaxation studies.[26] The data points included in the figure are derived from the distribution functions displayed in Figure 2c. Three cutoff limits were chosen as 2.5, 2.6, and 2.7 nm and the number of bound molecules was calculated by integrating the distribution functions up to these limits. The proposed model provides a good description of the membrane–sugar interactions in the MD simulation. At low concentrations, the binding probability calculated from the simulations is high,

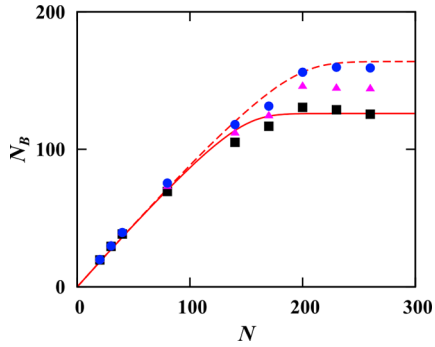

Figure 3. Number of bound molecules (N_B) as a function of the total number of TRH molecules (N). The lines are calculated using the membrane–sugar interaction model (eq 4) using the area per TRH molecule a_0 = 0.50 nm^2 (dashed) and a_0 = 0.65 nm^2 (solid). The points are derived from the TRH probability distribution functions in Figure 2c using cutoff values: 2.5 nm (squares), 2.6 nm (triangles), and 2.7 nm (circles).

close to 0.9, and also fairly constant, as predicted by the model and consistent with the binding hypothesis. At a certain concentration, however, the model predicts that the bound phase (the membrane) gets saturated, and any new TRH molecule that is added to the system will end up in the free phase, the solution. In the simulations, the value at which N_B levels off is strongly dependent on the somewhat arbitrary value for the cutoff.

We have attempted to approximate the different distributions in Figure 2c using Gaussian functions, but for high TRH concentrations the number of Gaussians became prohibitively high. Interestingly, the area covered by the TRH molecules is $N_B \times a_0 = 133 \times 0.65 \approx 86$ nm^2, very similar to the total lipid area $N_L \times A_L = 128 \times 0.64 \approx 82$ nm^2, where N_L is the number of lipids in the bilayer. Clearly, the complete coverage corresponds to one trehalose molecule per lipid.

At this point, we will compare our results with the recently published experimental study,[4] where membrane–trehalose interactions were investigated. In that work, the affinity of trehalose to the DMPC bilayer was determined using dialysis measurements. The net affinity is defined as $\Gamma = (N_B - N_F)/N_L = (2N_B - N)/N_L$, where $N_F = N - N_B$ is the number of free TRH molecules. The affinity profile derived from the membrane–sugar interaction model is shown in Figure 4 together with the points calculated from the MD trajectories. The analogy between Figures 3 and 4 can also be pointed out: the squares in both figures correspond to the same data points from the MD simulations and likewise the red solid profiles were calculated using the same set of parameters. The maximum affinity predicted by the model and calculated from the MD simulation is 0.65 and 0.55 TRH molecules/lipid, respectively, which corresponds to one sugar for each 1–2 lipids. This maximum occurs at w^F_{TRH} = 0.05 (w/w) free trehalose which gives a concentration of 0.15 M. The deviation between the model and simulation results increases at higher TRH content, which may be associated with the fact that the model does not include explicit TRH–TRH interactions.

The experimentally determined affinity points,[4] included in Figure 4, exhibit a maximum at w^F_{TRH} = 0.06 (w/w) with Γ = 0.07, i.e., one bound sugar for each 14 lipids. The experimental concentration of the free TRH at the maximum affinity is 0.2 M, which is very similar to our value of 0.15 M. In the dialysis measurements[4] the lipid concentration was 20–60 mmol lipid/

dx.doi.org/10.1021/jp402385d | J. Phys. Chem. B 2013, 117, 6667–6673

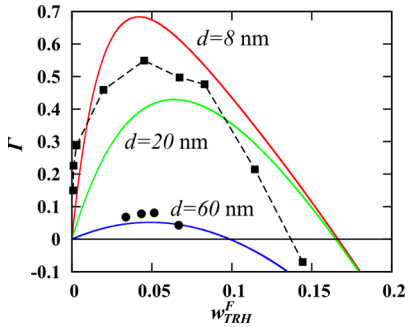

Figure 4. Net affinity, $\Gamma = (2N_B - N)/N_L$, of trehalose for DMPC bilayer plotted as a function of the weight fraction of free trehalose, w^F_{TRH}. Solid squares (the dashed line is included to guide the eye) correspond to the MD simulations, whereas the affinity profiles are calculated from the interaction model and correspond to different sizes of the bulk phase: d = 8 nm, as in the MD simulations (red), d = 20 nm (green), and d = 60 nm (blue). Experimental net affinities from ref 4 are included (solid circles).

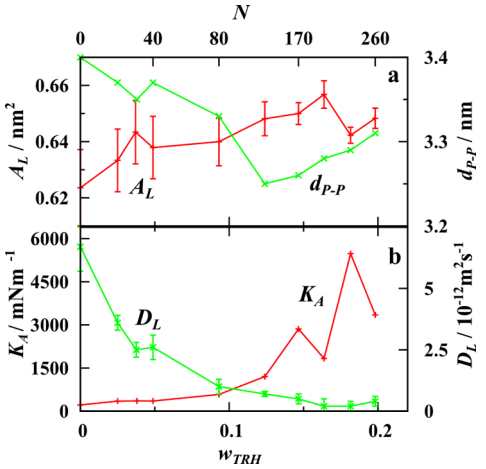

Figure 5. Trehalose concentration dependence of physical properties of the DMPC bilayer: (a) area per lipid (red); the bilayer thickness is represented by the distance between phosphorus atoms[33] in DMPC (green), and (b) area compressibility, K_A, for the lipid bilayer (red), and the lateral diffusion coefficient for DMPC (green). Note that w_{TRH} refers to the total TRH (w/w) concentration relative to all the components (TRH, lipids, and water).

(kg water), which approximately corresponds to 100 000 water molecules in our 128-lipid system. Thus, the water content (the size of the bulk) in the experiments is 1 order of magnitude higher compared with the MD simulations. Two affinity profiles calculated for larger bulks (increased values of the parameter d, thickness of the solvent layer; see Figure 1) are displayed in Figure 4. Clearly, the affinity approaches the experimental value upon increased water content. In fact, the d = 60 nm profile (blue line in Figure 4) is in very good agreement with the experimental points. The membrane–sugar interaction can also be characterized using the partition coefficient $P = [\mathrm{TRH}]_B/[\mathrm{TRH}]_F = z_B/z_F$, where z_B and z_F are numbers of particles in the bound and free regions, respectively. Using z_B = 43 nm and $z_F = d/2$ = 4 nm (see eq 1 and Figure 1 for the definition of these parameters), which correspond to MD simulations and are used for calculation of the red profile in Figure 4, gives $P \sim 10$ whereas the experimental value[4] is 0.6–2.5. Clearly, the difference between the partition coefficient and thus the free energy of transfer ($\Delta G^0 = -RT \ln P$) between the experimental and simulated systems originates almost exclusively from the 10 times larger bulk phase in the experiments.

The TRH concentration dependence of the area per lipid, A_L, and the average phosphorus–phosphorus distance, d_{P-P}, reflecting the membrane thickness are shown in Figure 5a. The area per lipid is an important parameter frequently used to characterize bilayers and to monitor phase transitions. The value of area per lipid for the reference system TRH0 is 0.62 ± 0.01 nm^2, which is in agreement with previously reported results for fully hydrated systems. The experimental values for the surface area of DMPC in membranes range from 0.58 to 0.67 nm^2 depending on the exact temperature and hydration level of the bilayer.[4,27−29] Previous molecular dynamics simulations of DMPC bilayers at 30 °C with 23 water molecules per lipid resulted in an area of 0.60 nm^2;[30] A_L for 25 water molecules at 40 °C was 0.63 nm^2, whereas a hydration level of 29 water molecules resulted in 0.63 and 0.65 nm^2 at 30 and 50 °C, respectively.[31] The addition of TRH results in an increase of A_L which can be interpreted as intercalation of the sugar molecules into the polar part of the bilayer. The penetration of the bilayer can also be observed in clearly asymmetric distribution functions for low TRH concentration samples in Figure 2c. At high concentrations of TRH the area per lipid becomes virtually constant at a level of 0.65 nm^2. The membrane thickness reflected in d_{P-P} decreases upon increased TRH content, which is consistent with the TRH intercalation and increased area per lipid that in turn leads to conformational changes in the chains, and therefore a decrease of the membrane thickness. Very similar results were obtained in a recent investigation[4] where the concept of intercalation was invoked for interpretation of small angle neutron scattering (SANS) and thermodynamic measurements. In contrast, however, earlier MD simulation of DPPC and trehalose mixtures[17,18] indicated an essentially unchanged spacing between the lipid headgroups. These simulations may be, as the authors pointed out, too short (10–15 ns) to observe bilayer–TRH interactions. The limited change of the area per lipid and the order parameters in the chains (Figure S1 of the Supporting Information) indicate that no phase transitions have occurred in our systems.

From the area per lipid and its fluctuations, the area compressibility modulus, K_A, can be calculated[32]

$$K_A = k_B T \langle A_L \rangle ((N_L/2)\langle (A_L - \langle A_L \rangle)^2 \rangle)^{-1} \quad (5)$$

where $\langle A_L \rangle$ is the average area per lipid. The TRH concentration dependence of the compressibility modulus is displayed in Figure 5b. A dramatic increase of the modulus with the TRH concentration is observed, which reflects increased rigidity of the membrane.

An opposite trend for K_A was reported[34] using an earlier version of the CHARMM force field. Simulations employing the latest version of CHARMM (C36) resulted, however, in an increased compressibility modulus upon addition of trehalose (R. W. Pastor and A. Sodt, private communication). The compressibility modulus for the reference sample TRH0 is 213 mN m^{-1}, which is in very good agreement with the experimental value of 234 ± 23 mN m^{-1}.[35] The compressibility modulus increases by more than 1 order of magnitude and becomes 6000 mN m^{-1} in TRH230. The error limits of K_A are, however, very large. It is so because the time scale of the area per lipid fluctuations is large compared to the simulation length and in addition depends on the system size.[36] At high TRH concentrations the fluctuations decrease and the time scale

dx.doi.org/10.1021/jp402385d | J. Phys. Chem. B 2013, 117, 6667−6673

increases which leads to extremely poor averaging. A significant increase of the area compressibility using the same force field as in the present work was observed upon addition of cholesterol to a DMPC bilayer[37] and in an experimental (X-ray diffraction) study[38] where a gel phase was formed. In the present study, there is no indication of gel phase formation (Figure S1 of the Supporting Information), but an increase of the lateral order is observed in the polar part of the bilayer. The high order in the membrane is also consistent with the decrease of the lateral diffusion coefficient, D_L, of the lipids (Figure 5b). Similarly, a strong effect of TRH on the lipid diffusion was observed in a 6 ns MD simulation of a DPPC bilayer.[21] The diffusion coefficient of DMPC in TRH0 is $(6.7 \pm 1.0) \times 10^{-12}$ m^2 s^{-1} (μm^2 s^{-1}) which is somewhat lower than the experimental values 16 and 9 μm^2 s^{-1} determined using pulsed field gradient (PFG) NMR spectroscopy[39] and fluorescence recovery after photobleaching (FRAP),[40] respectively. The drastic increase of the compressibility modulus and thus the membrane order upon increased TRH content is consistent with the vitrification hypothesis where a glassy state is formed that immobilizes membrane constituents. This immobilization is demonstrated in the lateral diffusion coefficients of the lipids (3.6 ± 0.3 and 0.4 ± 0.2 μm^2 s^{-1} for TRH20 and TRH260, respectively) and may be explained by extremely high local viscosity.[12] The (3-dimensional) diffusion of trehalose in the isotropic phase (800 ± 100 μm^2 s^{-1}) was derived from short MD simulations. A significant decrease in the lamellar phase was noted (10 μm^2 s^{-1}) where, in contrast to the diffusion of the lipids, only a weak concentration dependence was observed. We note that the TRH diffusion in the isotropic phase is slightly lower than experimentally observed and derived from MD simulations employing a CHARMM force field,[41] which may indicate higher TRH association in our system. According to the theory for membrane vitrification,[42] the elastic energies of membrane deformation and pore formation are proportional to the compressibility modulus. Thus, we can conclude that the mechanical properties of the bilayer undergo dramatic changes upon addition of trehalose. The vitrification has been associated with resistance to changes of the intracellular pH and ionic strength during dehydration.[11] The other hypothesis for membrane−sugar interaction rests on the assumption that carbohydrates replace water molecules at the bilayer interface.[7] This hypothesis is also confirmed by our results. In Figure 2d the distribution functions for water are displayed, which clearly indicate that water density at the interface decreases as the TRH concentration is increased.

CONCLUSIONS

Finally, we conclude that the present study confirms at least two of the hypotheses suggested for the explanation of the membrane−sugar interactions. We show, by calculating the net affinity of TRH for the DMPC bilayer, that the concept of attraction (low TRH content) and exclusion (high TRH content) of sugars from the membrane can be used in fully hydrated as well as in dehydrated membranes. The former situation was investigated in experimental thermodynamic studies,[4] whereas the latter refers to the present investigation. The net affinity in both systems has been calculated using a simple two-state model with the size of the water phase as the only variable. The calculated affinity profiles were in good agreement with experiments and computer simulations for both high and low TRH contents, supporting the attraction and exclusion concepts. Furthermore, the replacement of water by trehalose molecules is observed at the bilayer interface. Clearly, as previously suggested, the different hypotheses for membrane−sugar interactions are not mutually exclusive. The dramatically changed compressibility modulus and increased order, manifested by drastic reduction of the lateral diffusion, are attributed to formation of a glassy state in the less hydrated system.

METHODS

Molecular Dynamics Simulations. The DMPC topology is freely available online as the Supporting Information to ref 37. The trehalose topology was created using the GLYCAM Biomolecule Builder.[43] Starting configurations for the various concentrations were created using an equilibrated state of a previous concentration (starting with the DMPC reference, TRH0), removing water up to 0.3 nm from existing solutes (including DMPC) and adding new TRH molecules and water randomly to the empty space. The water content for the reference system, TRH0, as well as the four lowest TRH concentrations was 10 000 molecules, whereas approximately 14 000 water molecules were included in the other samples; see Table S1 of the Supporting Information.

The lipid interactions were modeled using a recently developed CHARMM based and AMBER compatible force field.[44] The TRH interaction parameters were GLYCAM06 based (also AMBER compatible),[45] and converted to GROMACS topology format using AnteChamber PYthon Parser interfacE (ACPYPE).[46] The TIP3P model was used for water interactions.[47]

All simulations were carried out in the NPT ensemble using the GROMACS v4.5.5 software package.[48] The temperature and pressure were controlled using the Nosé−Hoover thermostat[49,50] and the semianisotropic Parrinello−Rahman barostat[51] with coupling constants of 0.5 and 10 ps, respectively. The temperature was set to 310 K and the pressure to 100 kPa. Electrostatic interactions were calculated explicitly up to a cutoff distance of 1.0 nm, above which the interactions were treated using the particle mesh Ewald (PME) summation algorithm.[52] The nonbonded interactions were truncated at 1.3 nm and treated with a switch function from 1.2 nm. Dispersion correction for energy and pressure was turned on. The center of mass motion was removed in a linear fashion every integration step, individually for the upper and lower parts of the bilayer and the solvent grouped together with TRH. All bonds in water and solutes were constrained using the SETTLE[53] and LINCS algorithms,[54,55] respectively, and the simulations were performed using the leapfrog algorithm with a time step of 2 fs under periodic boundary conditions in orthorhombic boxes. A mixed scaling of 1−4 interactions was accomplished by a slight modification of the half-ϵ double pairlist method,[56] to fit the scalings of AMBER (0.8333) and GLYCAM06 (1.0). All the systems were equilibrated with a Berendsen[57] thermo- and barostat (with relaxation times of 0.1 and 1 ps, respectively) for 5 ns to stabilize the temperature and pressure before switching over to the production parameters. The systems were then equilibrated for at least 100 ns followed by the production simulations that lasted for 100−140 ns. Details about the simulations, including lengths of the production simulations, are presented in Table S1 in the Supporting Information.

Several short simulations of aqueous TRH solutions were carried out in order to investigate the TRH−TRH interactions. Strong indications of TRH cluster formation were observed

dx.doi.org/10.1021/jp402385d | J. Phys. Chem. B 2013, 117, 6667−6673

(based on the reorientational dynamics of TRH molecules; see Figure S2 of the Supporting Information), in agreement with recent experimental[26] and computational[58] results.

Potential of Mean Force. The PMFs were calculated by dragging two TRH molecules (one on each side of the bilayer) through the membrane using a penalty potential in one dimension. The TRH molecules retain their complete motional freedom except for the translational motion in the direction parallel to the normal of the bilayer that is constrained using an umbrella-type potential acting on the center of mass of the solute, with harmonic spring constants of 1000 kJ mol^{-1} nm^{-2}, and reference positions ranging from 0 to 4 nm from the center of the bilayer, in 0.05 nm increments. The resulting 81 simulations were run for 10 ns each, and the last 5 ns were included in the analysis. The weighted histogram method was employed for the PMF construction.[59] The reorientational dynamics investigated by the time correlation functions (TCFs) of TRH molecules for different distances from the bilayer center are displayed in Figure S3 of the Supporting Information.

■ ASSOCIATED CONTENT

Supporting Information

Orientational order parameters in acyl chains of DMPC and the reorientational dynamics of trehalose in the isotropic liquid and in the lipid bilayer are presented in figures together with simulation sample compositions compiled in a table. This material is available free of charge via the Internet at http://pubs.acs.org.

■ AUTHOR INFORMATION

Corresponding Author

*E-mail: arnold.maliniak@mmk.su.se.

Notes

The authors declare no competing financial interest.

■ ACKNOWLEDGMENTS

We thank Richard W. Pastor, Joakim Jämbeck, Alexander Lyubartsev, and Bertil Halle for valuable discussions. This work was supported by the Swedish Research Council (VR), the Carl Trygger Foundation, and the Swedish National Infrastructure for Computing (SNAC 001-12-102) via PDC (www.pdc.kth.se).

■ REFERENCES

(1) Tian, J.; Sethi, A.; Swanson, B. I.; Goldstein, B.; Gnanakaran, S. Taste of Sugar at the Membrane: Thermodynamics and Kinetics of the Interaction of a Disaccharide with Lipid Bilayers. *Biophys. J.* **2013**, *104*, 622−632.

(2) Crowe, L. M.; Reid, D. S.; Crowe, J. H. Is Trehalose Special for Preserving Dry Biomaterials? *Biophys. J.* **1996**, *71*, 2087−2093.

(3) Skibinsky, A.; Venable, R. M.; Pastor, R. W. A Molecular Dynamics Study of the Response of Lipid Bilayers and Monolayers to Trehalose. *Biophys. J.* **2005**, *89*, 4111−4121.

(4) Andersen, H. D.; Wang, C.; Arleth, L.; Peters, G. H.; Westh, P. Reconciliation of Opposing Views on Membrane-Sugar Interactions. *Proc. Natl. Acad. Sci. U.S.A.* **2011**, *108*, 1874−1878.

(5) Pereira, C. S.; Hünenberger, P. H. Effect of Trehalose on a Phospholipid Membrane under Mechanical Stress. *Biophys. J.* **2008**, *95*, 3525−3534.

(6) Crowe, J. H.; Crowe, L. M.; Chapman, D. Preservation of Membranes in Anhydrobiotic Organisms: the Role of Trehalose. *Science* **1984**, *223*, 701−703.

(7) López, C. A.; Rzepiela, A. J.; de Vries, A. H.; Dijkhuizen, L.; Hünenberger, P. H.; Marrink, S. J. Martini Coarse-Grained Force Field: Extension to Carbohydrates. *J. Chem. Theory Comput.* **2009**, *5*, 3195−3210.

(8) Lins, R. D.; Pereira, C. S.; Hünenberger, P. H. Trehalose-Protein Interaction in Aqueous Solution. *Proteins* **2004**, *55*, 177−186.

(9) Cottone, G.; Ciccotti, G.; Cordone, L. Protein−Trehalose−Water Structures in Trehalose Coated Carboxy-Myoglobin. *J. Chem. Phys.* **2002**, *117*, 9862−9866.

(10) Belton, P. S.; Gil, A. M. IR and Raman Spectroscopic Studies of the Interaction of Trehalose with Hen Egg White Lysozyme. *Biopolymers* **1994**, *34*, 957−961.

(11) Sun, W. Q.; Leopold, A. C. Cytoplasmic Vitrification and Survival of Anhydrobiotic Organisms. *Comp. Biochem. Physiol. Part A: Physiol.* **1997**, *117*, 327−333.

(12) Sun, W. Q.; Leopold, A. C.; Crowe, L. M.; Crowe, J. H. Stability of Dry Liposomes in Sugar Glasses. *Biophys. J.* **1996**, *70*, 1769−1776.

(13) Sun, W. Q.; Leopold, A. C. Glassy State and Seed Storage Stability: A Viability Equation Analysis. *Ann. Bot.* **1994**, *74*, 601−604.

(14) Crowe, J. H.; Crowe, L. M.; Carpenter, J. F.; Rudolph, A. S.; Wistrom, C. A.; Spargo, B. J.; Anchordoguy, T. J. Interactions of Sugars with Membranes. *Biochim. Biophys. Acta* **1988**, *947*, 367−384.

(15) Clegg, J. S. Cryptobiosis — a Peculiar State of Biological Organization. *Comp. Biochem. Physiol. B* **2001**, *128*, 613−624.

(16) Crowe, J. H.; Oliver, A. E.; Tablin, F. Is there a Single Biochemical Adaptation to Anhydrobiosis? *Integr. Comp. Biol.* **2002**, *42*, 497−503.

(17) Sum, A. K.; Faller, R.; de Pablo, J. J. Molecular Simulation Study of Phospholipid Bilayers and Insights of the Interactions with Disaccharides. *Biophys. J.* **2003**, *85*, 2830−2844.

(18) Villarreal, M. A.; Díaz, S. B.; Disalvo, E. A.; Montich, G. G. Molecular Dynamics Simulation Study of the Interaction of Trehalose with Lipid Membranes. *Langmuir* **2004**, *20*, 7844−7851.

(19) Pereira, C. S.; Lins, R. D.; Chandrasekhar, I.; Freitas, L. C. G.; Hünenberger, P. H. Interaction of the Disaccharide Trehalose with a Phospholipid Bilayer: a Molecular Dynamics Study. *Biophys. J.* **2004**, *86*, 2273−2285.

(20) Leekumjorn, S.; Sum, A. K. Molecular Investigation of the Interactions of Trehalose with Lipid Bilayers of DPPC, DPPE and Their Mixture. *Mol. Simul.* **2006**, *32*, 219−230.

(21) Pereira, C. S.; Hünenberger, P. H. The Influence of Polyhydroxylated Compounds on a Hydrated Phospholipid Bilayer: a Molecular Dynamics Study. *Mol. Simul.* **2008**, *34*, 403−420.

(22) Humphrey, W.; Dalke, A.; Schulten, K. VMD: visual molecular dynamics. *J. Mol. Graph.* **1996**, *14*, 33−38.

(23) Jónsdóttir, S. Ó.; Cooke, S. A.; Macedo, E. A. Modeling and measurements of solid-liquid and vapor-liquid equilibria of polyols and carbohydrates in aqueous solution. *Carbohydr. Res.* **2002**, *337*, 1563−1571.

(24) Kukol, A. Lipid Models for United-Atom Molecular Dynamics Simulations of Proteins. *J. Chem. Theory Comput.* **2009**, *5*, 615−626.

(25) Hansen, H. S.; Hünenberger, P. H. A Reoptimized GROMOS Force Field for Hexopyranose-Based Carbohydrates Accounting for the Relative Free Energies of Ring Conformers, Anomers, Epimers, Hydroxymethyl Rotamers, and Glycosidic Linkage Conformers. *J. Comput. Chem.* **2011**, *32*, 998−1032.

(26) Winther, L. R.; Qvist, J.; Halle, B. Hydration and Mobility of Trehalose in Aqueous Solution. *J. Phys. Chem. B* **2012**, *116*, 9196−9207.

(27) Costigan, S. C.; Booth, P. J.; Templer, R. H. Estimations of Lipid Bilayer Geometry in Fluid Lamellar Phases. *Biochim. Biophys. Acta* **2000**, *1468*, 41−54.

(28) Petrache, H. I.; Dodd, S. W.; Brown, M. F. Area per Lipid and Acyl Length Distributions in Fluid Phosphatidylcholines Determined by (2)H NMR Spectroscopy. *Biophys. J.* **2000**, *79*, 3172−3192.

(29) Nagle, J. F.; Tristram-Nagle, S. Structure of Lipid Bilayers. *Biochim. Biophys. Acta, Biomembr.* **2000**, *1469*, 159−195.

(30) Wohlert, J.; Edholm, O. Dynamics in Atomistic Simulations of Phospholipid Membranes: Nuclear Magnetic Resonance Relaxation Rates and Lateral Diffusion. *J. Chem. Phys.* **2006**, *125*, 204703.
(31) Högberg, C.-J.; Lyubartsev, A. P. A molecular Dynamics Investigation of the Influence of Hydration and Temperature on Structural and Dynamical Properties of a Dimyristoylphosphatidylcholine Bilayer. *J. Phys. Chem. B* **2006**, *110*, 14326−14336.
(32) Marrink, S. J.; Mark, A. E. Effect of Undulations on Surface Tension in Simulated Bilayers. *J. Phys. Chem. B* **2001**, *105*, 6122−6127.
(33) Kapla, J.; Stevensson, B.; Dahlberg, M.; Maliniak, A. Molecular Dynamics Simulations of Membranes Composed of Glycolipids and Phospholipids. *J. Phys. Chem. B* **2012**, *116*, 244−252.
(34) Venable, R. M.; Skibinsky, A.; Pastor, R. W. Constant Surface Tension Molecular Dynamics Simulations of Lipid Bilayers with Trehalose. *Mol. Simul.* **2006**, *32*, 849−855.
(35) Rawicz, W.; Olbrich, K. C.; McIntosh, T.; Needham, D.; Evans, E. Effect of Chain Length and Unsaturation on Elasticity of Lipid Bilayers. *Biophys. J.* **2000**, *79*, 328−339.
(36) Poger, D.; Mark, A. E. On the Validation of Molecular Dynamics Simulations of Saturated and cis-Monounsaturated Phosphatidylcholine Lipid Bilayers: A Comparison with Experiment. *J. Chem. Theory Comput.* **2010**, *6*, 325−336.
(37) Jämbeck, J. P. M.; Lyubartsev, A. P. Another Piece of the Membrane Puzzle: Extending Slipids Further. *J. Chem. Theory Comput.* **2013**, *9*, 774−784.
(38) Tristram-Nagle, S.; Liu, Y.; Legleiter, J.; Nagle, J. F. Structure of Gel Phase DMPC Determined by X-Ray Diffraction. *Biophys. J.* **2002**, *83*, 3324−3335.
(39) Orädd, G.; Lindblom, G.; Westerman, P. W. Lateral Diffusion of Cholesterol and Dimyristoylphosphatidylcholine in a Lipid Bilayer Measured by Pulsed Field Gradient NMR Spectroscopy. *Biophys. J.* **2002**, *83*, 2702−2704.
(40) Almeida, P. F.; Vaz, W. L.; Thompson, T. E. Lateral Diffusion in the Liquid Phases of Dimyristoylphosphatidylcholine/Cholesterol Lipid Bilayers: a Free Volume Analysis. *Biochemistry* **1992**, *31*, 6739−6747.
(41) Venable, R. M.; Hatcher, E.; Guvench, O.; Mackerell, A. D.; Pastor, R. W. Comparing Simulated and Experimental Translation and Rotation Constants: Range of Validity for Viscosity Scaling. *J. Phys. Chem. B* **2010**, *114*, 12501−12507.
(42) Voinova, M. V. The Theory of Membrane "Vitrification". *Thermochim. Acta* **1996**, *280*−*281*, 465−477.
(43) Woods Group. (2005−2012) Glycam Web. Complex Carbohydrate Research Center, University of Georgia, Athens, GA (http://www.glycam.com).
(44) Jämbeck, J. P. M.; Lyubartsev, A. P. Derivation and Systematic Validation of a Refined All-Atom Force Field for Phosphatidylcholine Lipids. *J. Phys. Chem. B* **2012**, *116*, 3164−3179.
(45) Kirschner, K. N.; Yongye, A. B.; Tschampel, S. M.; González-Outeiriño, J.; Daniels, C. R.; Foley, B. L.; Woods, R. J. GLYCAM06: A Generalizable Biomolecular Force Field. Carbohydrates. *J. Comput. Chem.* **2008**, *29*, 622−655.
(46) Sousa da Silva, A. W.; Vranken, W. F. ACPYPE - AnteChamber PYthon Parser interfacE. *BMC Res. Notes* **2012**, *5*, 367.
(47) Jorgensen, W. L.; Chandrasekhar, J.; Madura, J. D.; Impey, R. W.; Klein, M. L. Comparison of Simple Potential Functions for Simulating Liquid Water. *J. Chem. Phys.* **1983**, *79*, 926−935.
(48) Hess, B.; Kutzner, C.; van der Spoel, D.; Lindahl, E. GROMACS 4: Algorithms for Highly Efficient, Load-Balanced, and Scalable Molecular Simulation. *J. Chem. Theory Comput.* **2008**, *4*, 435−447.
(49) Nosé, S. A Unified Formulation of the Constant Temperature Molecular Dynamics Methods. *J. Chem. Phys.* **1984**, *81*, 511−519.
(50) Hoover, W. Canonical dynamics: Equilibrium Phase-Space Distributions. *Phys. Rev., A* **1985**, *31*, 1695−1697.
(51) Parrinello, M.; Rahman, A. Polymorphic Transitions in Single Crystals: A New Molecular Dynamics Method. *J. Appl. Phys.* **1981**, *52*, 7182−7190.
(52) Essmann, U.; Perera, L.; Berkowitz, M. L.; Darden, T.; Lee, H.; Pedersen, L. G. A Smooth Particle Mesh Ewald Method. *J. Chem. Phys.* **1995**, *103*, 8577−8593.
(53) Miyamoto, S.; Kollman, P. A. Settle: An Analytical Version of the SHAKE and RATTLE Algorithm for Rigid Water Models. *J. Comput. Chem.* **1992**, *13*, 952−962.
(54) Hess, B.; Bekker, H.; Berendsen, H. J. C.; Fraaije, J. G. E. M. LINCS: A Linear Constraint Solver for Molecular Simulations. *J. Comput. Chem.* **1997**, *18*, 1463−1472.
(55) Hess, B. P-LINCS: A Parallel Linear Constraint Solver for Molecular Simulation. *J. Chem. Theory Comput.* **2008**, *4*, 116−122.
(56) Chakrabarti, N.; Neale, C.; Payandeh, J.; Pai, E. F.; Pomès, R. An Iris-Like Mechanism of Pore Dilation in the CorA Magnesium Transport System. *Biophys. J.* **2010**, *98*, 784−792.
(57) Berendsen, H. J. C.; Postma, J. P. M.; van Gunsteren, W. F.; DiNola, A.; Haak, J. R. Molecular Dynamics with Coupling to an External Bath. *J. Chem. Phys.* **1984**, *81*, 3684−3690.
(58) Sapir, L.; Harries, D. Linking Trehalose Self-Association with Binary Aqueous Solution Equation of State. *J. Phys. Chem. B* **2011**, *115*, 624−634.
(59) Kumar, S.; Rosenberg, J. M.; Bouzida, D.; Swendsen, R. H.; Kollman, P. A. The Weighted histogram Analysis Method for Free-Energy Calculations on Biomolecules. I. The Method. *J. Comput. Chem.* **1992**, *13*, 1011−1021.